# Distribution of Off-Diagonal Cross Sections in Quantum Chaotic Scattering: Exact Results and Data Comparison

Santosh Kumar, Barbara Dietz, Thomas Guhr, and Achim Richter

Phys. Rev. Lett. **119**, 244102 — Published 13 December 2017

DOI: 10.1103/PhysRevLett.119.244102

# Distribution of Off-Diagonal Cross Sections in Quantum Chaotic Scattering: Exact Results and Data Comparison

Santosh Kumar,[1,*] Barbara Dietz,[2,†] Thomas Guhr,[3,‡] and Achim Richter[4,§]

[1]*Department of Physics, Shiv Nadar University, Gautam Buddha Nagar, Uttar Pradesh 201314, India*
[2]*School of Physical Science and Technology, and Key Laboratory for Magnetism and Magnetic Materials of MOE, Lanzhou University, Lanzhou, Gansu 730000, China*
[3]*Fakultät für Physik, Universität Duisburg-Essen, Lotharstraße 1, D-47048 Duisburg, Germany*
[4]*Institut für Kernphysik, Technische Universität Darmstadt, D-64289 Darmstadt, Germany*

The recently derived distributions for the scattering-matrix elements in quantum chaotic systems are not accessible in the majority of experiments, whereas the cross sections are. We analytically compute distributions for the off-diagonal cross sections in the Heidelberg approach, which is applicable to a wide range of quantum chaotic systems. We thus eventually fully solve a problem which already arose more than half a century ago in compound-nucleus scattering. We compare our results with data from microwave and compound-nucleus experiments, particularly addressing the transition from isolated resonances towards the Ericson regime of strongly overlapping ones.

*Introduction.* — Scattering experiments are indispensable to understand the microscopic world. Mainly developed in nuclear physics [1–10], scattering theory now finds various applications in condensed matter physics [11–14], in classical wave systems [15–17], in wireless communication [18] and other fields [19–21]. An incoming wave in a scattering channel $b$, say, is modified in the scattering zone, *e.g.*, by a nucleus as the target, and leaves it through a scattering channel $a$. The elements $S_{ab}(E)$ of the associated scattering matrix $S$ are complex numbers. They provide all information on the changes in amplitude and phase, typically with energy $E$. The $S$ matrix is unitary due to flux conservation and its dimension coincides with the number $M$ of channels. In a few cases both the modulus and the phase of the $S$-matrix elements can be measured directly, *e.g.*, in experiments with microwave cavities, microwave networks or reverberating elastic objects [22–25]. In the majority of scattering experiments, particularly in quantum physics, the phase is not accessible. In mesoscopic quantum dots [26] the electron transport, that is, the conductance is measured instead, of which the fluctuations are well understood [13, 14, 27, 28]. In a scattering experiment involving quantum particles, *i.e.*, atoms [29–32], molecules [33, 34] or nuclei [35], only the incoming and outgoing particle current can be measured. Their ratio yields the cross sections. For $a \neq b$ they are given by

$$\sigma_{ab}(E) = |S_{ab}(E)|^2 = \left(\mathrm{Re}\, S_{ab}(E)\right)^2 + \left(\mathrm{Im}\, S_{ab}(E)\right)^2 . \quad (1)$$

This formula might have to be supplemented with multiplicative factors of purely kinematic origin.

If the dynamics in the scattering zone is sufficiently complex or, in a rather general sense, chaotic, scattering can usually be thought of as a random process [36]. There are in principle two stochastic approaches to chaotic scattering [8, 13]. In the Mexico approach [37, 38], the $S$ matrix as a whole is viewed as a random matrix, whereas in the Heidelberg approach randomness is assumed for the Hamiltonian $H$ describing the internal dynamics in the interaction region. While the former has an unrivaled conceptual elegance, the latter is better suited for grasping important features of the internal dynamics since the scattering process as such is fully modeled on the microscopic level.

We have three goals: First, we calculate within the Heidelberg approach the exact distribution of the off-diagonal cross sections $\sigma_{ab}$ with $a \neq b$, corresponding to inelastic scattering or rearrangement collisions, thereby providing the complete solution of a long-standing problem. It applies from the regime of isolated resonances with average resonance width $\Gamma$ smaller than the average resonance spacing $D$, *i.e.*, $\Gamma/D \ll 1$, all the way up to the Ericson regime [39] of strongly overlapping resonances, $\Gamma/D \gg 1$. Second, we test our results by comparing with cross-section data obtained in microwave and compound-nucleus experiments, focussing on the transition to the Ericson regime. Third, we provide a simple and robust method to extract non-random contributions to the cross-section distribution.

*Scattering matrix.* — The Heidelberg approach [40, 41] is based on [5]

$$S_{ab}(E) = \delta_{ab} - i2\pi W_a^\dagger G(E) W_b \,, \quad (2)$$

$$G^{-1}(E) = E\mathbb{1}_N - H + i\pi \sum_{c=1}^{M} W_c W_c^\dagger \,, \quad (3)$$

where $G(E)$ is the matrix resolvent. The widths of the resonances generated by the poles of $G(E)$ in the complex energy plane exhibit non-trivial fluctuations [42]. They are controlled by the interplay between the Hamilton matrix $H$ describing the scattering zone and the coupling vectors $W_c$ which account for the interaction between the channels $c$ and the states of $H$.

Scattering can involve different time scales. In nuclear physics, there are direct, non-random reactions on very short time scales due to channel-channel coupling. On longer time scales a compound nucleus is formed by the

target and the incoming particles. Its equilibration ensures a sufficient amount of stochasticity, justifying the replacement of $H$ by a random matrix. We assume absence of direct coupling between the channels, implying that the coupling vectors $W_c$ may be chosen orthogonal, $W_c^\dagger W_d = \gamma_c \delta_{cd}/\pi$ [41, 43] where $\gamma_c$ is referred to as partial width. Depending on whether the system is time-reversal invariant or noninvariant, $H$ either belongs to the Gaussian Orthogonal Ensemble (GOE) or to the Gaussian Unitary Ensemble (GUE) [8, 44] designated by the Dyson indices $\beta = 1$ and $\beta = 2$, respectively. The entries of the matrices $H$ are Gaussian distributed, $\mathcal{P}(H)d[H] \sim \exp\left(-\frac{\beta N}{4v^2}\mathrm{tr}H^2\right) d[H]$ with variance parameter $v^2$. The flat measure $d[H]$ is the product of differentials of all independent elements in the $N \times N$ matrix $H$. All physical quantities are measured on the local scale of the mean level spacing. This implies universality, *i.e.*, a very large class of probability densities gives the same result in the limit $N \to \infty$; see Refs. [8, 44].

*Cross-section distribution.* — Although the cross-section distribution was of high interest already in the early days of compound-nucleus and, more generally, of chaotic scattering, it continued to resist an analytical solution [45]. In a seminal work using the supersymmetry method, Verbaarschot, Weidenmüller and Zirnbauer [40] derived the exact two–point energy correlation function of the $S$-matrix elements. Davis and Boosé calculated three- and four-point correlation functions [46, 47] and Fyodorov, Savin and Sommers the distribution of the diagonal $S$-matrix elements [48]. Rozhkov, Fyodorov, and Weaver [49, 50] computed a related quantity, namely the statistics of transmitted power. Putting forward a new variant of the supersymmetry method, we recently calculated the distributions of the real and the imaginary parts of the off–diagonal $S$ matrix [51, 52]. In a related study, Fyodorov and Nock obtained the distributions of off–diagonal elements of the Wigner $K$ matrix [53]. Nevertheless, the cross-section distribution remained out of reach, because the cross section (1) depends on the real and imaginary parts of the $S$-matrix element which are not independent. Thus, to compute it for $a \neq b$,

$$p(\sigma_{ab}) = \int_{-\infty}^{\infty} dx_1 \int_{-\infty}^{\infty} dx_2 \, \delta(\sigma_{ab} - x_1^2 - x_2^2) P(x_1, x_2) \ , \tag{4}$$

the knowledge of the joint probability density function

$$P(x_1, x_2) = \int d[H] \mathcal{P}(H) \delta(x_1 - \mathrm{Re}\, S_{ab}) \delta(x_2 - \mathrm{Im}\, S_{ab}) \tag{5}$$

is inevitable. At first sight, one might expect that this task leads to doubling the size of the supersymmetric non–linear sigma model as compared to Refs. [48, 51, 52], rendering further evaluation forbiddingly complicated. However, we recently discovered that a simple, yet far-reaching modification and generalization of our supersymmetry technique in Refs. [51, 52] yields $P(x_1, x_2)$ without enlarging this size.

*Joint probability density.* — It turns out to be advantageous to employ the Fourier transform, *i.e.*, the bivariate characteristic function

$$R(k_1, k_2) = \int d[H] \mathcal{P}(H) e^{-ik_1 \,\mathrm{Re}\, S_{ab} - ik_2 \,\mathrm{Im}\, S_{ab}} \tag{6}$$

in two dimensions, such that

$$P(x_1, x_2) = \frac{1}{4\pi^2} \int_{-\infty}^{\infty} dk_1 \int_{-\infty}^{\infty} dk_2 \, e^{ik_1 x_1 + ik_2 x_2} R(k_1, k_2) \, . \tag{7}$$

Anticpating the data analysis to follow we emphasize that the characteristic function is obtained by sampling from the experimental data as easily as the joint probability density itself. With Eq. (7) in Eq. (4) and the complex variables $\mathbf{k} = k_1 + ik_2$ and $\mathbf{x} = x_1 + ix_2$, we find

$$p(\sigma_{ab}) = \frac{1}{4\pi^2} \int d^2\mathbf{x} \int d^2\mathbf{k} \, \delta(\sigma_{ab} - |\mathbf{x}|^2) e^{i \,\mathrm{Re}\,(\mathbf{k}^* \mathbf{x})} R(\mathbf{k}) \ . \tag{8}$$

The $\mathbf{x}$ integrals can be done with polar coordinates,

$$p(\sigma_{ab}) = \frac{1}{4\pi} \int d^2\mathbf{k} \, R(\mathbf{k}) \, J_0\big(\sqrt{\sigma_{ab}}|\mathbf{k}|\big) \ , \tag{9}$$

expressing the cross-section distribution as a certain Bessel transform of the characteristic function. The crucial step to make the calculation of the latter feasible is to use Eq. (3) in Eq. (6) in the form

$$R(\mathbf{k}) = \int d[H] \mathcal{P}(H) \exp\big(-i\pi W^T A \, W\big) \tag{10}$$

with the $2N$ component vector $W^T = [W_a^T, W_b^T]$ for $a \neq b$, and the $2N \times 2N$ Hermitian matrix

$$A = \begin{bmatrix} 0 & -i\mathbf{k}^* G \\ i\mathbf{k} G^\dagger & 0 \end{bmatrix} \tag{11}$$

in terms of the resolvent in Eq. (3). In Refs. [51, 52] we proceeded similarly, but for marginal distributions and thus univariate characteristic functions that depend either on $k_1$ or on $k_2$. Absorbing them as complex variable $\mathbf{k}$ into the definition of $A$ preserves its Hermiticity. Hence, we may adjust all further steps in Refs. [51, 52] by moving the calculation into the complex $\mathbf{k}$ plane. We introduce bosonic integrals for a Fourier transform of the characteristic function (10) in $W$ space to invert the resolvent $G$ in $A$. A thereby occurring determinant is written as a fermionic integral. This allows us to do the ensemble average over the random matrices $H$ exactly. We obtain a supermatrix model that we bring onto the local scale by a saddlepoint approximation for $N \to \infty$. This yields a supersymmetric nonlinear sigma model extending the one in Refs. [51, 52]. Details are given in Sect. I of the supplemental material [54].

For $\beta = 2$ with unitarily invariant $H$ the final result for the characteristic function is

$$R(\mathbf{k}) = 1 - \int_1^\infty d\lambda_1 \int_{-1}^1 d\lambda_2 \frac{|\mathbf{k}|^2}{4(\lambda_1-\lambda_2)^2}\, \mathcal{F}_{\rm U}(\lambda_1,\lambda_2) \times \left(t_a^1 t_b^1 + t_a^2 t_b^2\right) J_0\left(|\mathbf{k}|\sqrt{t_a^1 t_b^1}\right) , \qquad (12)$$

with the channel factor

$$\mathcal{F}_{\rm U}(\lambda_1,\lambda_2) = \prod_{c=1}^{M} \frac{g_c^+ + \lambda_2}{g_c^+ + \lambda_1} , \qquad (13)$$

where $t_c^j = \sqrt{|\lambda_j^2 - 1|}/(g_c^+ + \lambda_j)$, and $g_c{}^\pm = (v^2 \pm \gamma_c^2)/(\gamma_c\sqrt{4v^2 - E^2})$. The parameter $g_c^+$ is related to the transmission coefficient or the sticking probability $T_c = 1 - |S_{cc}|^2$ as $g_c^+ = 2/T_c - 1$. The remarkable fact that the characteristic function (12) depends only on $|\mathbf{k}|$ implies that the distribution of real and imaginary parts of $S_{ab}$ are identical [51, 52] for $\beta = 2$. For $\beta = 1$ with orthogonally invariant $H$ we arrive at

$$R(\mathbf{k}) = 1 + \frac{1}{8\pi}\int_{-1}^1 d\lambda_0 \int_1^\infty d\lambda_1 \int_1^\infty d\lambda_2 \int_0^{2\pi} d\psi \times \mathcal{J}(\lambda_0,\lambda_1,\lambda_2)\mathcal{F}_{\rm O}\left(\lambda_0,\lambda_1,\lambda_2\right)\left(\kappa_1+\kappa_2+\kappa_3+\kappa_4\right) . \qquad (14)$$

The Jacobian in the above expression is given by

$$\mathcal{J} = \frac{(1-\lambda_0^2)|\lambda_1-\lambda_2|}{2(\lambda_1^2-1)^{1/2}(\lambda_2^2-1)^{1/2}(\lambda_1-\lambda_0)^2(\lambda_2-\lambda_0)^2} , \qquad (15)$$

and the channel factor reads

$$\mathcal{F}_{\rm O}(\lambda_0,\lambda_1,\lambda_2) = \prod_{c=1}^{M} \frac{g_c^+ + \lambda_0}{(g_c^+ + \lambda_1)^{1/2}(g_c^+ + \lambda_2)^{1/2}} . \qquad (16)$$

The $\kappa$'s in Eq. (14) depend on $g_c^\pm$ and the complex $\mathbf{k}$ in a nontrivial way; see Sect. II of the supplemental material [54].

*Comparison with microwave data.* — The mathematical equivalence of spectra of two–dimensional quantum billiards and flat microwave resonators is used to experimentally explore a variety of quantum chaotic phenomena in closed [22, 23, 55, 56] and open systems [57–63]. Here, we use the data measured for a microwave billiard in the shape of a classically chaotic tilted–stadium billiard; see Refs. [62–64] for experimental details. The $S$-matrix elements $S_{ab}$ were measured in steps of 100 kHz in a range from 1 to 25 GHz. Their fluctuation properties were evaluated in frequency windows of 1 GHz to guarantee a negligible secular variation of the coupling vectors $W_c$. In Ref. [51] we analyzed the marginal distributions of real and imaginary parts of $S_{ab}$ and the corresponding univariate characteristic functions separately. We now compare our new analytical results for the joint probability density $P(x_1, x_2)$, for the bivariate characteristic function $R(k_1, k_2)$ and for the cross section distribution $p(\sigma_{ab})$ with these data. Figure 1 shows the bivariate characteristic function in the frequency range 10-11 GHz. Plotted are the analytical and experimental results together. The same comparison is shown in Fig. 2 for the frequency range 24-25 GHz; see also Fig.1 of the supplemental material [54]. The agreement is very good in both cases. For the lower frequencies, the peak is broad and heavy–tailed, corresponding to a non-Gaussian joint probability density. For the higher ones, the peak is narrow and Gaussian–like, yielding the joint probability density with a nearly Gaussian shape for the frequency range 24-25 GHz, displayed in Fig. 3. To explain these results, we point out that the system undergoes with increasing frequency a transition from isolated resonances to largely overlapping ones, *i.e.*, to the onset region of the Ericson regime [64]. For the frequency ranges 10-11 GHz and 24-25 GHz, we have $\Gamma/D = 0.23$ and $\Gamma/d = 1.21$, respectively. In the Ericson regime, scattering matrices and cross sections are random functions and the peaks in the spectra cannot be associated with particular resonances, implying that the distribution of the $S$-matrix elements is Gaussian [3, 41]. According to Eq. (4), the distribution of normalized cross sections is then exponential with $p(0) = 1$. To test this, we also compare in Fig. 4 our results for the distribution of cross sections normalized to

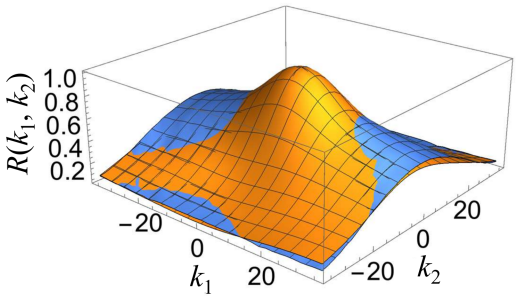


FIG. 1: Bivariate characteristic function $R(k_1, k_2)$ in the frequency range 10-11 GHz. Analytical result (blue) and microwave data (orange).

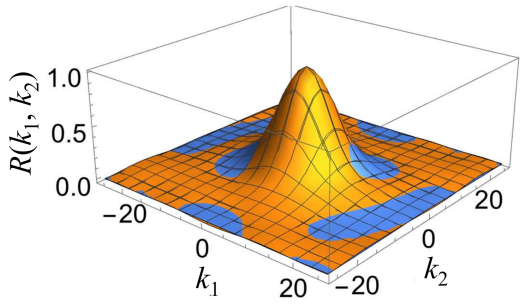


FIG. 2: As Fig. 1, but in the frequency range 24-25 GHz.

their mean with the data. As seen, our exact results compare well to all regimes including the transition region. The nearly exponential form with $p(0) > 1$ in the frequency range 24-25 GHz clearly indicates that we are in the onset of the Ericson regime.

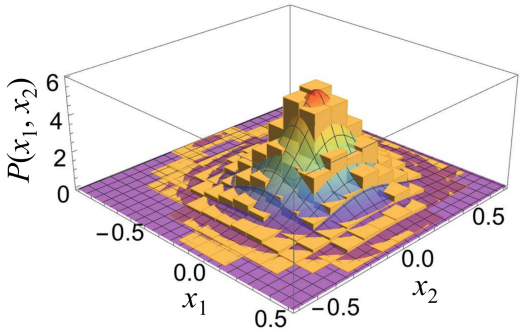


FIG. 3: Joint probability density $P(x_1, x_2)$, analytical (surface) and microwave data (histogram) in the frequency range 24-25 GHz.

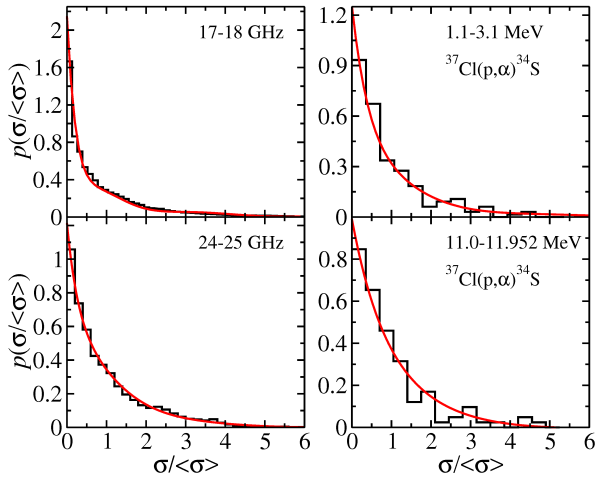


FIG. 4: Distribution of normalized cross sections. Experimental data as histograms from microwave (left) and nuclear experiments (right), respectively. Analytical results as solid red lines.

*Comparison with compound-nucleus data.* — We also use data from historical measurements of the compound-nuclear reaction $^{37}$Cl(p,$\alpha$)$^{34}$S [65–67]. In Ref. [66], excitation functions were measured in steps of 8 keV in the proton-energy range 11-11.952 MeV for 12 scattering angles between 31° to 175°. Importantly, these data are fully in the Ericson regime with $\Gamma/D \approx 27 - 36$. In Fig. 5 we show a selection of three such excitation functions for 31°, 110° and 175°. At smaller angles, one observes a background, *i.e.*, a nonzero minimum value of the excitation function. It is due to direct reactions, in which, *e.g.*, an incoming particle kicks out an $\alpha$ particle without formation of a compound nucleus. As such processes are stronger in forward than in backward direction, the background disappears at larger angles. In addition, they are barely affected by the chaotic dynamics in the scattering zone and thus cannot be random. Hence, their energy dependence is marginal and we may safely substract the background to obtain the fluctuating compound-nuclear contribution. In Fig. 4 we compare the distribution of normalized cross-sections, *i.e.*, $p(\sigma/\langle\sigma\rangle)$ obtained from the 175° measurement with the analytical prediction. For this, we use $M = 5$ (effective) open channels and all transmission coefficients $T_c = 0.99$ in accordance with Ref. [66], leading to an exponential. We find a very good match.

To complete our studies we, furthermore, apply our analytical results to nuclear data in the region of weakly overlapping resonances. In Ref. [68], the reaction $^{37}$Cl(p,$\alpha$)$^{34}$S was measured in the proton-energy range 1.1-3.1 MeV at a scattering angle of 90°. These data, shown in Fig. 6, exhibit an unusually sharp increase at an energy of approximately 2.6 MeV which is due to experimental imperfections. We thus restrict the data analysis to the energy range 1.1-2.6 MeV. The background stemming from the direct reactions is a smoothly increasing function of energy, hence subtracting it is more involved than in the previously considered case; see Fig. 5. This reflects a general problem in analyzing compound-nuclear data. Unfortunately, we cannot exploit recent progress that has been made employing the $K$ matrix [69, 70], since it relies on the knowledge of the $S$-matrix elements. Instead, we put forward a seemingly new empirical method which is based on the observation that the peak exhibited by the cross-section distribution of compound-nuclear reactions at $\sigma = 0$ is shifted to a nonzero value by direct contributions. Thus, we fit the excitation function below 2.6 MeV with a second-order polynomial, which we then subtract from the data. This leads to the experimental cross-section distribution displayed in Fig. 4 which is peaked at zero. Our analytical result is very well capable of describing this clearly non-exponential distribution for $M = 10$ effective channels and $T_c = 0.7$.

*Conclusions.* — We solved a long-standing problem by exactly calculating the distribution of the off-diagonal cross sections within the Heidelberg approach. This facilitates, for the first time, an analysis of distributions for the large number of systems, in which only the cross sections can be measured. We performed a detailed comparison with microwave and nuclear data, focusing on the transition from the regime of isolated resonances towards the Ericson regime. Our analytical results describe the data very well in all regimes. We are not aware of any comparable study for distributions and characteristic functions. In the course of our data comparison, we came up with a seemingly new and robust method to substract the direct part in cross-section data which only relies on experimental information.

We are grateful to A. Nock for his help in the ini-

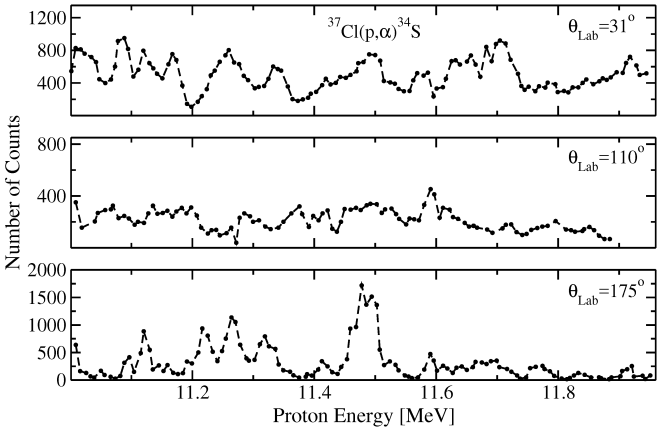


FIG. 5: Excitation functions for the reaction $^{37}$Cl(p,$\alpha$)$^{34}$S in the Ericson regime for scattering angles 31°, 110° and 175° from top to bottom. Digitized from Ref. [66].

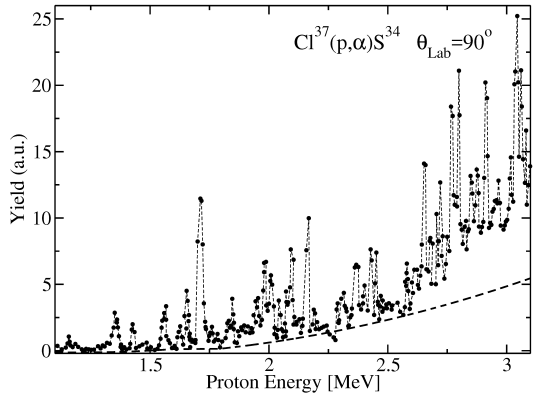


FIG. 6: Excitation functions for the reaction $^{37}$Cl(p,$\alpha$)$^{34}$S in below the Ericson regime for scattering angle 90°. Digitized from Ref. [68].

tial stages of this project, and to P. von Neumann-Cosel who helped us to find Ref. [68]. We acknowledge fruitful discussions with T. Kawano and H.A. Weidenmüller. SK also acknowledges the support by the grant EMR/2016/000823 provided by SERB, DST, Government of India. This work was supported by the Deutsche Forschungsgemeinschaft (DFG) within the Collaborative Research Centers 634 and 1245.

* Electronic address: skumar.physics@gmail.com
† Electronic address: dietz@lzu.edu.cn
‡ Electronic address: thomas.guhr@uni-due.de
§ Electronic address: richter@ikp.tu-darmstadt.de

[1] T. E. O. Ericson, Ann. Phys. (NY) **23**, 390 (1963).
[2] G. R. Satchler, Phys. Letters **7**, 55 (1963).
[3] D. M. Brink and R. O. Stephen, Phys. Lett. **5**, 77 (1963).
[4] C. E. Porter, *Statistical Theories of Spectra: Fluctuations* (Academic, New York, 1965).
[5] C. Mahaux and H.A. Weidenmüller, *Shell Model Approach to Nuclear Reactions* (North Holland, Amsterdam, 1969).
[6] H. Feshbach, *Nuclear Reactions* (Wiley Classics Library, NY, 1993).
[7] V. Zelevinsky, Annu. Rev. Nucl. Part. Sci. **46**, 237 (1996).
[8] T. Guhr, A. Müller-Groeling, H. A. Weidenmüller, Phys. Rep. 299 (1998) 189.
[9] R. Pike, P. Sabatier (Eds.), *Scattering and Inverse Scattering in Pure and Applied Sciences* (Academic Press, NewYork, 2002).
[10] H. A. Weidenmüller and G. Mitchell, Rev. Mod. Phys. **81**, 539 (2009).
[11] P. A. Lee, A. Douglas Stone, and H. Fukuyama, Phys. Rev. B **35**, 1039 (1987).
[12] R. A. Jalabert, H. U. Baranger, and A. Douglas Stone, Phys. Rev. Lett. **65**, 2442 (1990).
[13] C. W. Beenakker, Rev. Mod. Phys. **69**, 731 (1997).
[14] Y. Alhassid, Rev. Mod. Phys. **69** 72, 895 (2000).
[15] R. L. Weaver, J. Acoust. Soc. Am. **85**, 1005 (1989).
[16] C. Ellegaard, T. Guhr, K. Lindemann, H. Q. Lorensen, J. Nygård, and M. Oxborrow, Phys. Rev. Lett. **75**, 1546 (1995).
[17] J.-B. Gros, O. Legrand, F. Mortessagne, E. Richalot, and K. Selemani, Wave Motion **51**, 664 (2014).
[18] R. Couillet and M. Debbah, *Random Matrix Methods for Wireless Communications* (Cambridge University Press, Cambridge, 2011).
[19] Y.V. Fyodorov, T. Kottos, H.-J. Stöckmann, J. Phys. A: Math. Gen. **38** (2005).
[20] G. E. Mitchell, A. Richter, and H. A. Weidenmüller, Rev. Mod. Phys. **82**, 2845 (2010).
[21] J.-H. Yeh, T. M. Antonsen, E. Ott, and S. M. Anlage, Phys. Rev. E **85**, 015202 (2012).
[22] H.-J. Stöckmann and J. Stein, Phys. Rev. Lett. **64**, 2215 (1990).
[23] H.-D. Gräf, H. L. Harney, H. Lengeler, C. H. Lewenkopf, C. Rangacharyulu, A. Richter, P. Schardt, and H. A. Weidenmüller, Phys. Rev. Lett. **69**, 1296 (1992).
[24] O. Hul, S. Bauch, P. Pakoński, N. Savytskyy, K. Życzkowski, and L. Sirko, Phys. Rev. E **69**, 056205 (2004).
[25] M. Avlund, C. Ellegaard, M. Oxborrow, T. Guhr, and N. Søndergaard, Phys. Rev. Lett. **104**, 164101 (2010).
[26] J. A. Folk, S. R. Patel, S. F. Godijn, A. G. Huibers, S. M. Cronenwett, and C. M. Marcus, Phys. Rev. Lett. **76**, 1699 (1996).
[27] H. A. Weidenmüller, Nucl. Phys. **A518**, 1 (1990).
[28] G. L. Celardo, F. M. Izrailev, S. Sorathia, V. G. Zelevinsky, and G. P. Berman, AIP Conf. Proc. **995**, 75 (2008).
[29] Jörg Main and Günter Wunner, Phys. Rev. Lett. **69**, 586 (1992).
[30] G. Stania and H. Walther, Phys. Rev. Lett. **95**, 194101 (2005).
[31] J. Madroñero and A. Buchleitner, Phys. Rev. Lett. **95**, 263601 (2005).
[32] A. Frisch, M. Mark, K. Aikawa, F. Ferlaino, J. L. Bohn, C. Makrides, A. Petrov, and S. Kotochigova, Nature (London) **507**, 475 (2014).
[33] S. A. Reid and H. Reisler, J. Chem. Phys. **100**, 474 (1996).
[34] M. Mayle, G. Quéméner, B. P. Ruzic, and J. L. Bohn, Phys. Rev. A **87**, 012709 (2013).

[35] T. E. O. Ericson and T. Mayer-Kuckuk, Annu. Rev. Nucl. Sci. **16**, 183 (1966).
[36] C. Jung, T. H. Seligman, Phys. Rep. **285**, 77 (1997).
[37] P. A. Mello, P. Pereya, and T. H. Seligman, Ann. Phys. **161**, 254 (1985).
[38] M. Martínez-Mares and P. A. Mello, Phys. Rev. E **72**, 026224 (2005).
[39] T. E. O. Ericson, Phys. Rev. Lett. **5**, 430 (1960).
[40] J. J. M. Verbaarschot, H. A. Weidenmüller and M. R. Zirnbauer, Phys. Rep. **129**, 367(1985).
[41] D. Agassi, H.A. Weidenmüller, G. Mantzouranis, Phys. Rep. **22**, 145 (1975).
[42] Y. V. Fyodorov and H.-J. Sommers, J. Math. Phys. **38**, 1918 (1997).
[43] C. H. Lewenkopf, H. A. Weidenmüller, Ann. Phys. **212**, 53 (1991).
[44] M. L. Mehta, *Random Matrices* (New York: Academic Press, 2004).
[45] T. E. O. Ericson, B. Dietz, and A. Richter, Phys. Rev. E **94**, 042207 (2016).
[46] E. D. Davis, D. Boosé, Phys. Lett. B **211**, 379 (1988).
[47] E. D. Davis, D. Boosé, Z. Phys. A **332**, 427 (1989).
[48] Y. V. Fyodorov, D. V. Savin, and H.-J. Sommers, J. Phys. A **38**, 10731 (2005).
[49] I. Rozhkov, Y. V. Fyodorov, and R. L. Weaver, Phys. Rev. E **68**, 016204 (2003).
[50] I. Rozhkov, Y. V. Fyodorov, and R. L. Weaver, Phys. Rev. E **69**, 036206 (2004).
[51] S. Kumar, A. Nock, H.-J. Sommers, T. Guhr, B. Dietz, M. Miski-Oglu, A. Richter, and F. Schäfer, Phys. Rev. Lett. **111**, 030403 (2013).
[52] A. Nock, S. Kumar, H.-J. Sommers, and T. Guhr, Ann. Phys. **342**, 103 (2014).
[53] Y. V. Fyodorov and A. Nock, J. Stat. Phys. **159**, 731 (2015).
[54] See Supplemental Material for more details concerning the derivation of the characteristic functions for the cases $\beta = 1, 2$, see Eqs. (12) and (14), and two additional figures showing the comparison between experimental and analytical results for the bivariate characteristic function and the joint probability distribution.
[55] S. Sridhar, Phys. Rev. Lett. **67**, 785 (1991).
[56] B. Dietz and A. Richter, CHAOS **25**, 097601 (2015).
[57] U. Kuhl, M. Martínez-Mares, R. A. Méndez-Sánchez, and H.-J. Stöckmann, Phys. Rev. Lett. **94**, 144101 (2005).
[58] U. Kuhl, H.-J. Stöckmann, and R. Weaver, J. Phys. A: Math. Gen. **38**, 10433 (2005).
[59] S. Hemmady, X. Zheng, T. M. Antonsen, E. Ott, and S. M. Anlage, Phys. Rev. E **71**, 056215 (2005).
[60] O. Hul, O. Tymoshchuk, S. Bauch, P. M. Koch, and L. Sirko, J. Phys. A: Math. Gen. **38**, 10489 (2005).
[61] M. Ławniczak, O. Hul, S. Bauch, P. Sěba, and L. Sirko, Phys. Rev. E **77**, 056210 (2008).
[62] B. Dietz, T. Friedrich, H. L. Harney, M. Miski-Oglu, A. Richter, F. Schäfer, J. Verbaarschot, and H. A. Weidenmüller, Phys. Rev. Lett. **103**, 064101 (2009).
[63] B. Dietz, T. Friedrich, H. L. Harney, M. Miski-Oglu, A. Richter, F. Schäfer, and H. A. Weidenmüller, Phys. Rev. E **81**, 036205 (2010).
[64] B. Dietz, H. L. Harney, A. Richter, F. Schäfer, and H. A. Weidenmüller, Phys. Lett. B **685**, 263 (2010).
[65] P. von Brentano, J. Ernst, O. Häusser, T. Mayer-Kuckuk, A. Richter, and W. von Witsch, Phys. Lett. **9**, 48 (1964).
[66] W. von Witsch, P. von Brentano, T. Mayer-Kuckuk, and A. Richter, Nucl. Phys. **80**, 394 (1966).
[67] A. Richter, A. Bamberger, P. von Brentano, T. Mayer-Kuckuk, and W. von Witsch, Z. Naturforschg. **21a**, 1001 (1966).
[68] R. L. Clarke, E. Almqvist. and E. B. Paul, Nucl. Phys. **14**, 472 (1959).
[69] T. Kawano, P. Talou, and H. A. Weidenmüller, Phys. Rev. C **92**, 044617 (2015).
[70] T. Kawano, R. Capore, S. Hilaire, and P. Chau Huu-Tai, Phys. Rev. C **94**, 014612 (2016).